Submitted for the 5th International Conference on Deformation and Fracture of Composites, 18-19 March,1999, London

Fatigue damage in carbon fibre reinforced aluminium alloy laminates

T S P Austin[1], P J Gregson[1], J P Dakin[2], P.M. Powell[3] and M M Singh[1]

[1] Department of Engineering Materials, University of Southampton

[2] Optoelectronics Research Centre, University of Southampton

[3] Structural Materials Centre, Defence Evaluation & Research Agency, Farnborough

Abstract

This research seeks to develop a unified model for fatigue crack and damage growth processes in a hybrid laminate. The progress of damage in a carbon fibre reinforced aluminium alloy laminate has been monitored, while simultaneously the strain within a defined area in the vicinity of the crack has been measured directly, by means of fibre optic sensors. Some preliminary finite element modelling results are presented. It is shown that the range of the stress intensity factor remains the most significant parameter for characterising fatigue crack growth. A stress intensity factor, modified to account for the changing compliance introduced by fibre-bridging and delamination, was found to be appropriate for these materials.

Introduction

Hybrid laminates typically consist of alternate fibre reinforced polymer and aluminium alloy laminae. Developed primarily for fatigue-critical aerospace applications, i.e. fuselage and lower wing skins, the hybrid laminates are orthotropic materials of lower density and higher strength than the simple aluminium alloy monolith. The response of the hybrid laminate to fatigue cracking about fastener holes is of particular design interest. The behaviour is typically one of fatigue cracking confined to the alloy laminae, and delamination between the composite and alloy layers[1-6]. Although there is deterioration of the integrity of the FRP laminae in the vicinity of the fatigue crack, there is a tendency for the reinforcing carbon fibre to 'bridge' the flanks of the crack, hence improving the resistance to fatigue crack growth (FCG) by restraining the opening of the crack in the aluminium alloy layer.

We present a method of mapping the strain field within the FRP layer of a carbon fibre reinforced aluminium alloy (CARALL) subjected to fatigue damage initiated at a through-thickness fastener hole. A two-dimensional array of optical fibre sensors consisting of in-fibre Bragg gratings has been embedded within the composite. These sensors are periodic variations in the refractive index of the fibre core, that make narrowband reflective filters that are "tuned" by mechanical strain. A multiplexed system for the interrogation of the peak reflective wavelength of the Bragg-grating strain sensors was constructed. This system was based on a broadband source and an acousto-optic tunable filter to determine the peak grating wavelength[7-10]. We have been able to relate the progress of delamination to the strain field in the vicinity of the crack. A finite element model has been developed to simulate the

experimental conditions, with the ultimate aim of producing a unified model for fatigue crack and damage growth processes in a hybrid laminate.

Experimental methods

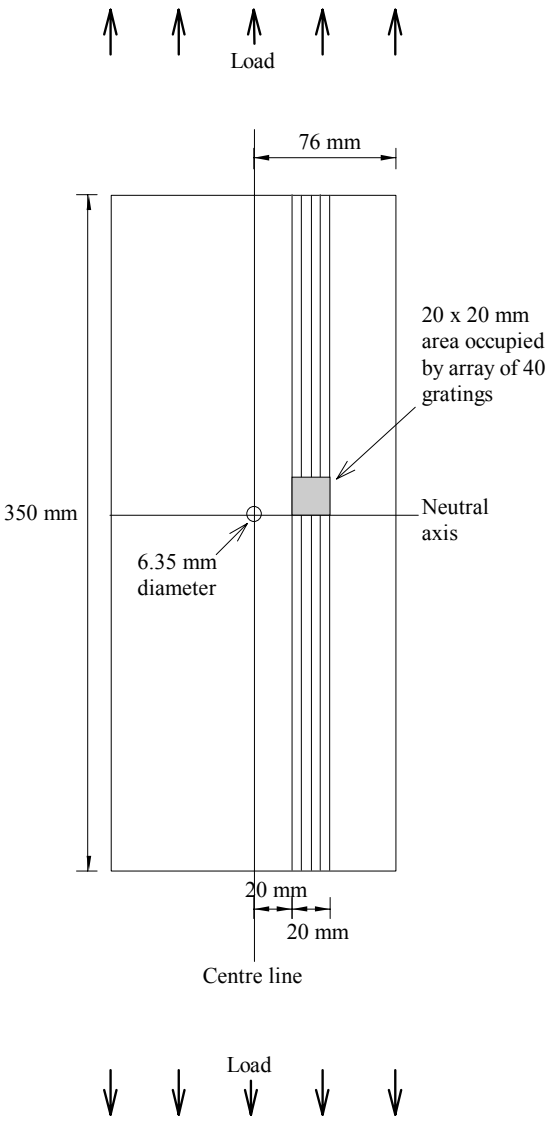

Figure 1. M(T) panel configuration with embedded optical fibres (broken lines).

FCG studies were performed on M(T) specimens[11], made from four carbon fibre reinforced epoxy plies (913C HTA) of total thickness 0.5 mm, sandwiched between 0.48 mm thick 8090 aluminium-lithium alloy skins. All panels were unidirectional, with both the carbon fibres and the original rolling direction of the aluminium alloy aligned along the loading axis. Five fibre-optic lines, each identically equipped with eight sensors of different wavelength, were embedded 5 mm apart in the centre of the carbon fibre plies, parallel to the carbon fibres (Figure 1). The panels were cured in an autoclave at 120°C. The optical fibres were located such that the array of forty gratings occupied a 20 x 20 mm square area immediately adjacent to the expected path of crack propagation (the shaded area in Figure 1). On each optical fibre line, the gratings were located 1mm, 2mm, 3mm, 4mm, 6mm, 8mm, 12mm and 20mm, respectively, from the neutral axis.

The sample was cyclically loaded with a sinusoidal wave-form at a frequency of 10 Hz in a servo-hydraulic machine. Crack length and load-line displacement were logged continuously, using a pulsed direct current potential drop (DCPD) method and a clip gauge, respectively. The test was interrupted at intervals, and a 'dry' ultrasonic C-scanner was used to record the delamination zone, while the panel remained in the test machine.

The interrogation system was configured to track individual gratings for a period of 1.1 seconds, at a sampling frequency of approximately 200 Hz. To monitor the entire grid required a total period of about 90 seconds. Compared with the extended duration of the complete fatigue crack growth test (typically 7 days) this generated an essentially instantaneous record of strain across the 20 x 20 mm area over which the gratings were

distributed. The maximum and minimum strain of each cycle were logged, readings being made automatically every 200s, and the strain amplitude was calculated.

A number of panels were tested, and details of the test conditions for each panel are given below:

Panel No.	R-ratio	ΔP (kN)	Width (mm)	Thickness (mm)	Optical fibres
8H9	0.1	18	152.50	1.43	5 (interrogation system not operational)
8H10	0.1	18	152.84	1.47	5 (only one functional)
8H14	0.1	25	152.88	1.48	5
8H15	0.5	18	152.74	1.42	5

Results and Discussion

Fatigue crack growth

The fatigue crack growth data for the laminates presented in Figure 2 illustrates the improvement in performance gained by introducing the CFRP layer into the aluminium alloy.

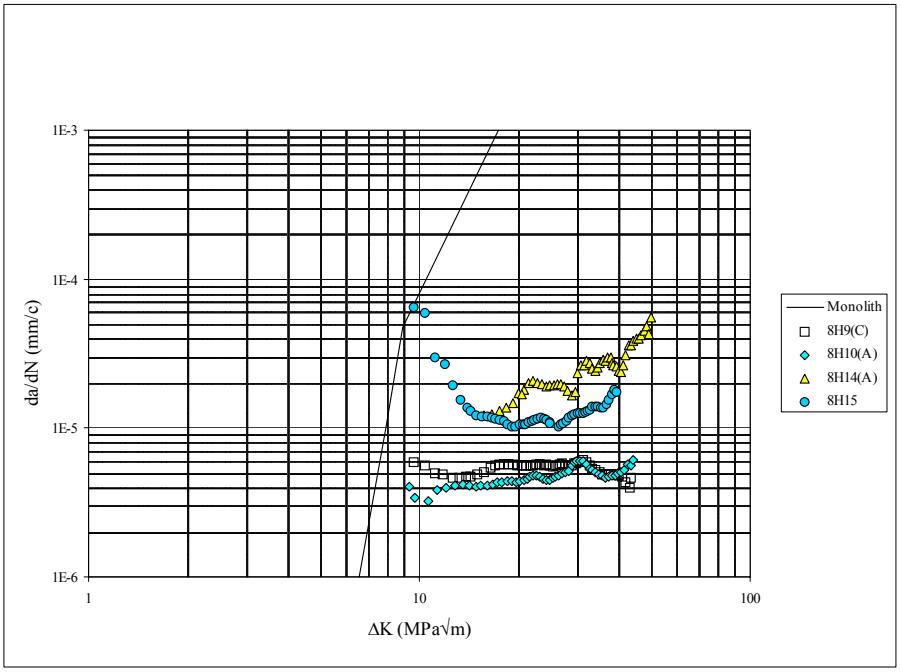

Figure 2. Fatigue crack growth versus stress intensity factor range, ΔK(laminate), for 4-ply CARALL laminates under different loading conditions

An effective value for the stress intensity factor range in the alloy skins, $\Delta K_{eff}(Al)$, was calculated to account for the effects of fibre-bridging and load partitioning. The assumption was made that the measured compliance incorporated all components of the FCG process.

From the measured crack length, the stress intensity factor range for the laminate was calculated according to the ASTM method[11], assuming that the laminate was a uniform material. The rule of mixtures was then applied to evaluate the load applied to the skins, and hence, the stress intensity factor for the skins, $\Delta K(Al)$. From measurements of the crack opening displacement and applied load, the compliance of the laminate was measured. This was compared to the theoretical compliance derived from the standard ASTM compliance function for the given crack length. The fibres bridging the crack flanks increase the stiffness of the panel, so that the measured compliance is less than the theoretical value. The ratio of the measured to theoretical compliance values defines the fraction of the applied load acting upon the crack, so that the effective ΔK applied to the crack, $\Delta K_{eff}(Al)$, can then be determined. Figure 3 details crack growth data as a function of $\Delta K_{eff}(Al)$ for the test panels.

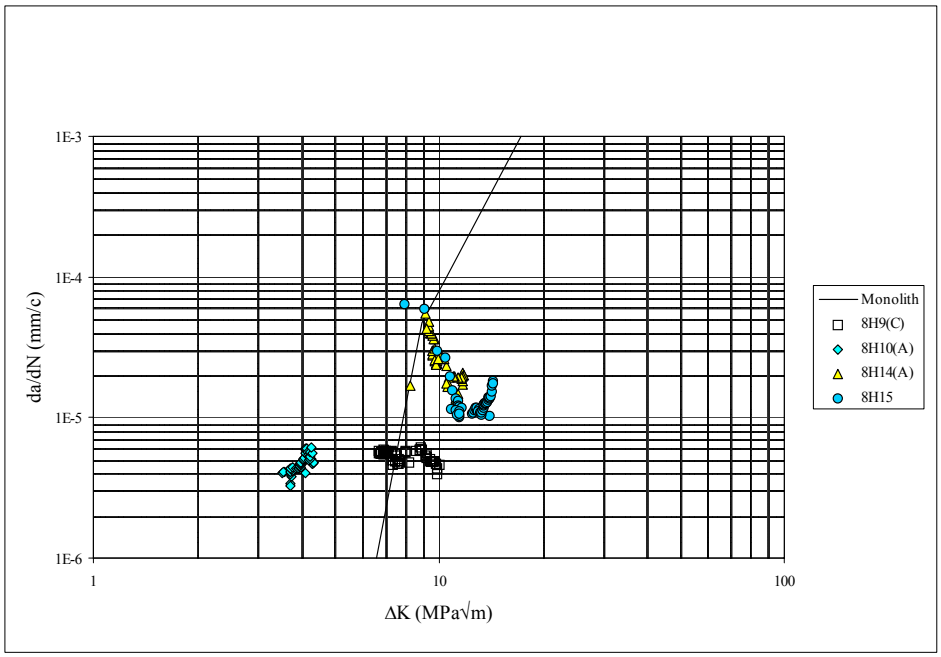

Figure 3. Fatigue crack growth versus effective stress intensity factor range, $\Delta K_{eff}(Al)$, for 4-ply CARALL laminates

The correlation of laminate FCG rates with monolithic behaviour is considerably improved, although the data appear to display a degree of clustering, as opposed to simple scatter.

Typical development of delamination is shown in Figure 4. In this instance, three ultrasonic scans were performed after 1102361, 1713276 and 2598694 cycles, respectively. The unbroken lines represent the boundary of the delamination zones between the front alloy skin and the composite, while the dashed lines depict the rear zones. The typical triangular shape[3] is clear, and this tends to become more elliptical[4] as delamination progresses. It can be seen that the damage is asymmetric, both left and right about the vertical axis, and front and rear. The nature of the asymmetry differed from one specimen to another, and appears to be caused by small variations in the materials and in loading configurations.

The relative positions of the optical fibres and their gratings are also shown in Figure 4. The growth of the delaminated area can be compared with the development of the strain amplitude. For example, Figure 5 shows the strain amplitude recorded for Line 1 (at a horizontal distance x = 20 mm from the central hole). Each trace represents the strain

amplitude at a grating, with the grating a distance y = 1 mm from the neutral axis indicating the onset of delamination first. The delamination boundaries did not reach the grating at y = 20 mm, so the lowermost trace shows only small changes in strain amplitude.

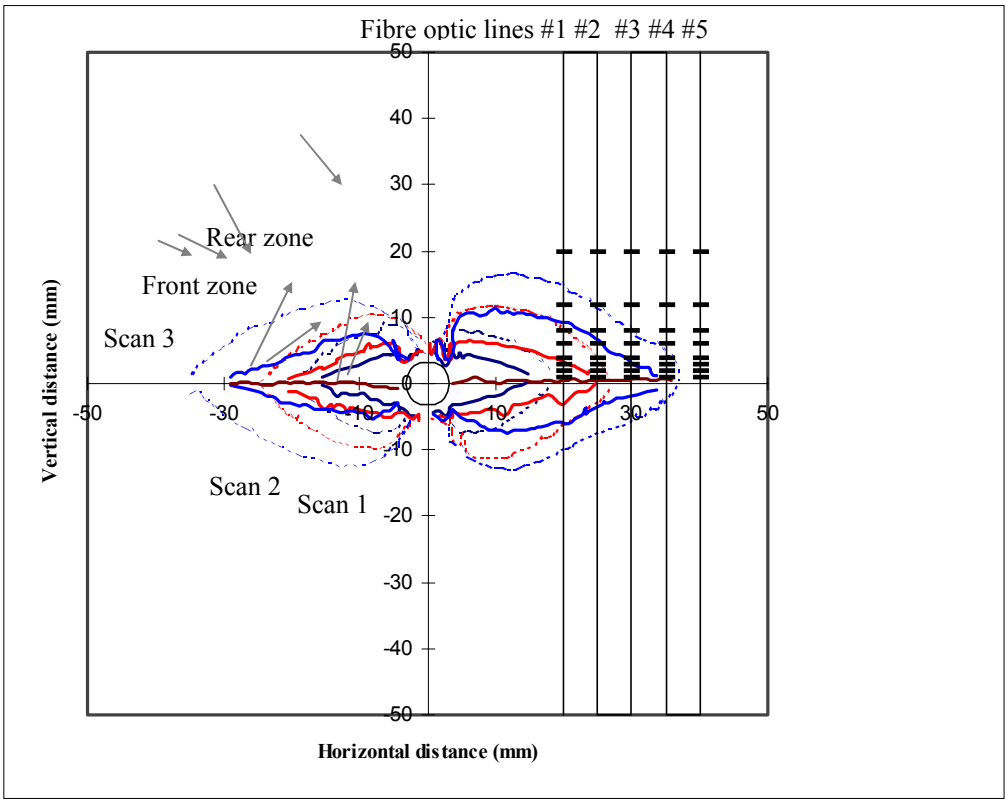

Figure 4. Development of delaminated regions within a 4-ply CARALL laminate (panel 8H15) subject to fatigue.

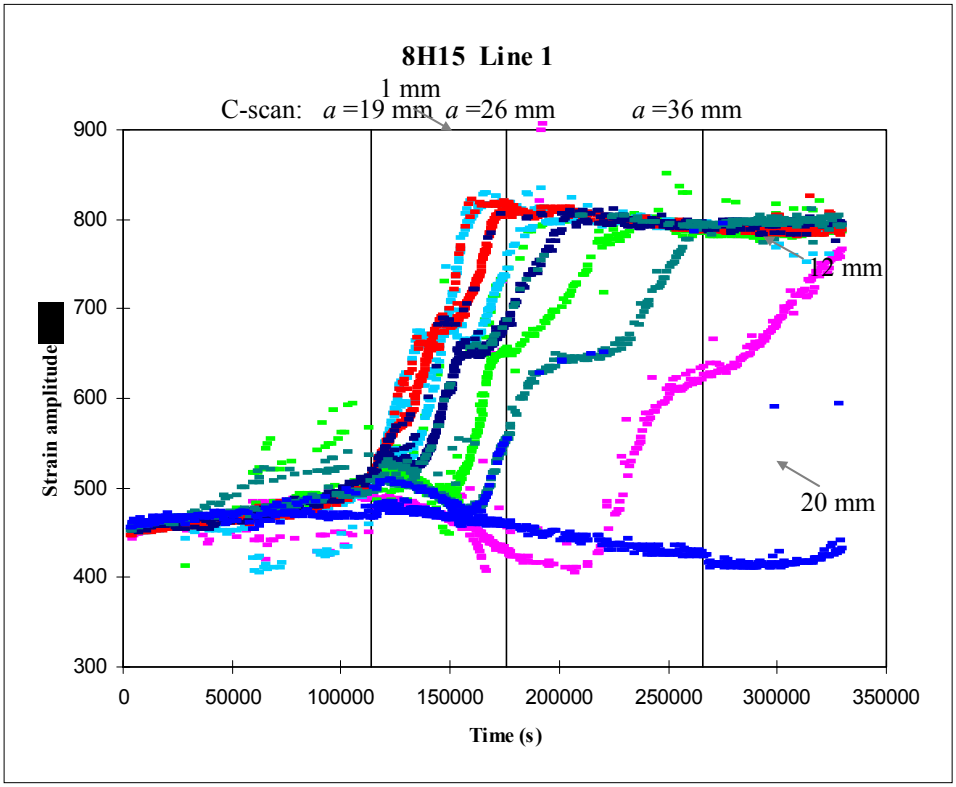

Figure 5. Strain amplitude data from fibre optic line #1 as a function of time for a CARALL laminate (panel 8H15)

Worthy of note are the two plateaux, a short one at about 650 με and the other the stable peak value of approximately 800 με. The presence of the first is due to a mismatch in the delamination profile either side of the composite ply, such that there is a delay between the boundaries of each delamination passing across a particular sensor. The second plateau is reached when the material has delaminated on both sides of the grating.

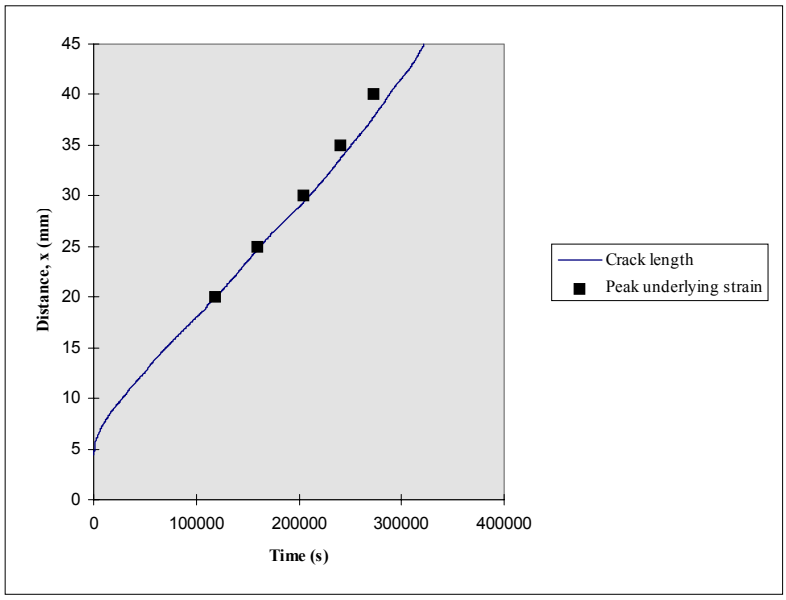

Figure 6. Comparison of progress of the crack tip and the peak in the underlying strain.

In Figure 5, a maximum in the underlying strain is observed just before the rapid increase in strain amplitude is apparent in the first grating. In Figure 6, the progress of this maximum is

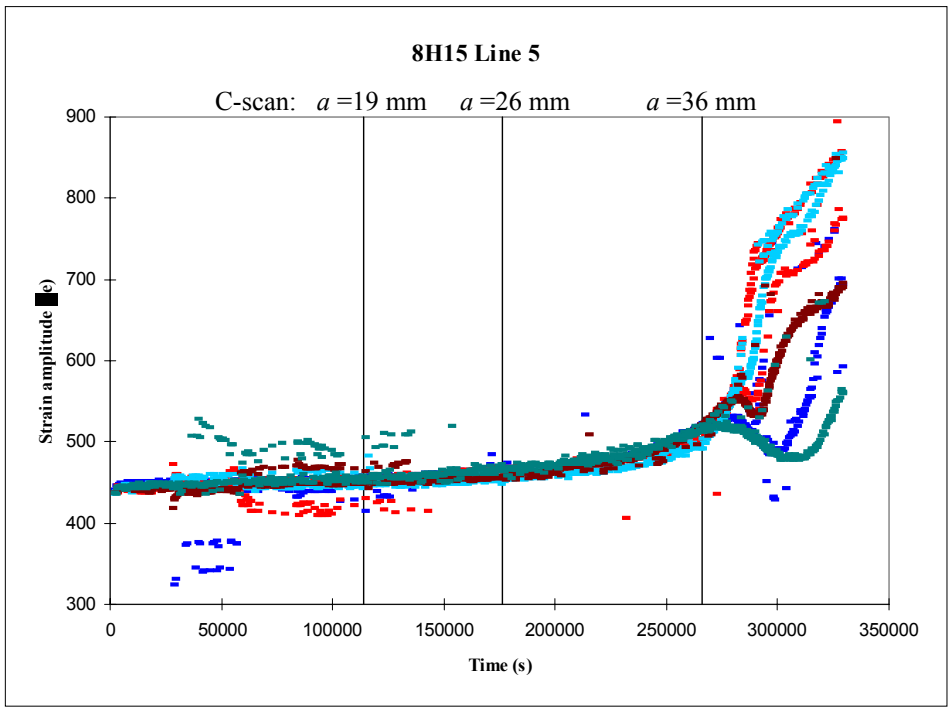

Figure 7. Strain amplitude data from fibre optic line #5 as a function of time, for a CARALL laminate

compared with the crack growth. The strain amplitude reaches this peak just ahead of the crack tip, but the time lag increases as the crack grows. The magnitude of the peak decreases with vertical distance from the crack, and, as illustrated in Figure 5, the underlying strain amplitude relaxes once the crack tip has passed the optical fibre. This suggests that the peak in strain amplitude is a consequence of the stress concentration ahead of the crack tip being transferred into the composite, even though there is no corresponding crack in the CFRP. The continued reduction in strain amplitude to a value below the initial value, evident at 12 mm above the crack, would imply a redistribution of the load within the composite, a greater portion being carried by the edges, i.e. as might be expected to take place if fibre breakage occurred within the crack wake. Correspondingly, the strain amplitude at Line 5 (situated at x = 40 mm from the centre of the panel) showed a steady gradual increase, as the crack tip approached, as shown in Figure 7, in which only 6 traces are shown, for clarity.

Some "noise" is evident in the optical fibre data and this problem is currently being addressed. However, the trends are clear, and a direct quantitative measure of the strain amplitude has also been obtained.

Finite element modelling

Numerical simulation of the observed failure mechanism has been achieved by incorporating the measured delamination profiles into finite element analyses (FEA) performed using the public domain package FRANC2DL[12]. Figure 8 details the mesh generated from a measured delamination zone.

All our FEA analysis was based on the assumption that the cracks are confined to the alloy skins, and that fibre bridging occurs along the length of the crack. Due to software

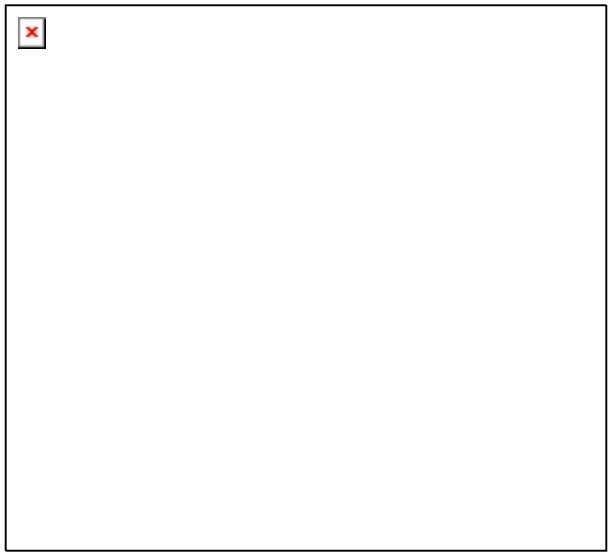

Figure 8. Typical FEA mesh generated using measured delamination data

limitations, preliminary numerical studies have assumed isotropic CFRP properties. Numerical simulation of the system has allowed the relative effects of the various components of the hybrid laminate FCG mechanism to be investigated. The individual failure processes that constitute hybrid laminate FCG include fibre bridging, delamination, loss of CFRP stiffness, and mismatch between the delamination zone front and the crack tip. When predicted results are compared with experimental records, good correlation is apparent between the ΔK_{eff}(Al) data set and the predicted data (Figure 9). The s = 0 data set assumes that the delamination boundary is coincident with the crack tip, and that there is no reduction in CFRP stiffness. The data set labelled s ~ 0.6 incorporates a mismatch of approximately 0.6 mm between the delamination zone front and the crack tip, as well as a 20% loss of stiffness across an area coincident with the delamination.

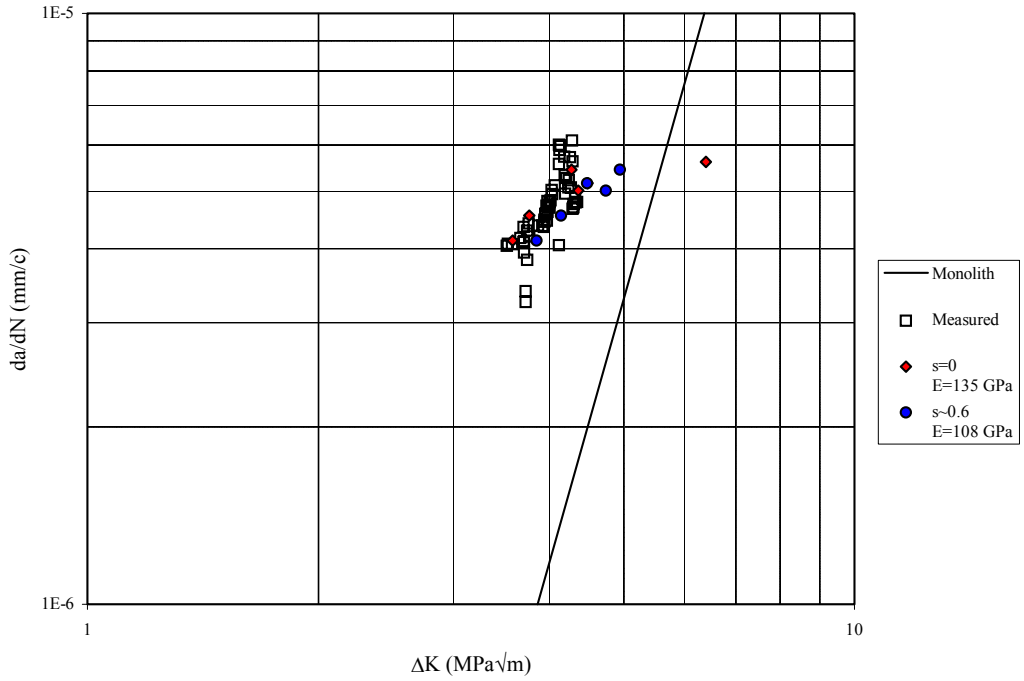

Figure 9. Comparison of measured and experimental $\Delta K_{(eff)}$(Al) for a 4-ply CARALL laminate (panel 8H10)

Analysis shows that incorporating a mismatch, s ~ 0.6 alone, with no loss of stiffness, reduces the predicted ΔK; Figure 9 indicates that the loss of stiffness causes an increase in predicted ΔK. However, the data suggest that these details of the failure process are second order effects.

An early analysis predicted the rise in underlying strain in the CFRP observed ahead of the crack tip, and that the strain would attain a plateau within the delaminated zone. Our ongoing analysis will be aimed at achieving a more precise comparison of the predicted and experimental strain fields.

Conclusions

A means of directly measuring the internal strain within the composite layer of a CARALL hybrid laminate has been demonstrated. The observed changes in the strain field have been related to both crack growth and delamination between the composite and the alloy skins.

Finite element analysis has shown that the loss of stiffness in the composite and the spatial lag between the crack tip and the delamination boundary are secondary effects. An effective value of stress intensity factor in the aluminium alloy, based on compliance measurements, has been shown to be an important factor governing the rate of fatigue crack growth.

Acknowledgement

This investigation was carried out for DERA under EMR agreement SMCFU/772. The support of the Ministry of Defence and the Department of Trade and Industry is gratefully acknowledged. The authors wish to thank L. Reekie, M. Cole and M. Durkin for provision of in-fibre gratings during the course of the work.

References

1. Marissen R, Engineering Fracture Mechanics 19 (1984) 261
2. Ritchie R O, Weikang Yu, & Bucci R J, Engineering Fracture Mechanics 32 (1989) 361
3. Lin C T, Kao P W & Yang F S, Composites 22 (1991) 135
4. Lin C T & Kao P W, Materials Science & engineering A190 (1995) 65
5. Lin C T & Kao P W, Composites Part A 27A (1996) 9
6. Davenport S B, Gregson P J, Moreton R & Peel C J, Journal of Materials Science 32 (1997) 6555
7. Xu M G, Geiger H, Archambault J L, Reekie L & Dakin J P, Electronic Letters 29 (1993) 1510
8. Xu M G, Geiger H, Archambault J L, Reekie L & Dakin J P, Electronic Letters 30 (1994) 1085
9. Geiger H, Xu M G, Eaton N C & Dakin J P, Electronic Letters 31 (1995) 1006
10. Volanthen M, Geiger H, Xu M G & Dakin J P, Electronic Letters 32 (1996) 1228
11. ASTM E 647-95A 'Annual Book of ASTM Standards', Section 3 (1996) 565
12. James M & Swenson D, FRANC2D/L: A Crack Propagation Simulator for Plane Layered Structures, at *http://www.engg.ksu.edu/~franc2d/*